Sarat chandra Kuchibhatla & Devesh Ranjan (dranjan@tamu.edu)
Department of Mechanical Engineering, Texas A&M University, College Station, TX, 77843-3123

Understanding the impact of initial conditions on low Atwood number Rayleigh-Taylor driven flows

Rayleigh-Taylor Instability (RTI): Background

- Classical fluid instability observed when density gradient and pressure gradient are misaligned, i.e. $\nabla p . \nabla \rho < 0$.
- Evolution through three main stages: Linear growth rate stage of initial perturbations, non-linear growth stage where saturation is observed, and transition to turbulence where self-similar growth is observed.
- Governing parameter of the flow, Atwood number, $A_t = (\rho_{heavy} - \rho_{light})/(\rho_{heavy} + \rho_{light})$ and Reynolds number based on mixing width, $Re_{mix} = (gA_t/6)^{0.5} (2h)^{1.5}/\nu$, where ρ is density, g is gravity, $2h$ is mixing width and ν is kinematic viscosity. The Water channel experiments have a low A_t of the order of 10^{-3} and Re_{mix} of about 1300.
- Schematic of the experimental setup is shown in fig. 1 below, with components labeled. The top and bottom convective streams of water have a mean speed of 4.7cm/s each, without any shear between the streams. The splitter plate is of 0.32cm thickness, and the channel test-section has dimensions of $L \times B \times H = 48in \times 13in \times 18in$.
- Effects of multi-modal initial conditions (ICs) on RTI are studied using a high-accuracy, servo-controlled, flapper-mechanism (fig. 2), which generates a multi-modal waveform at the fluid interface, given by $y = 0.1\Sigma \; \lambda_i \sin(\omega_i t + \beta_{i-1})$, where y is the perturbation, λ_i is the i-th mode's wavelength, ω_i is the i-th frequency, and β_{i-1} is the phase-angle with respect to the first mode. The amplitude to wavelength ratio of 0.1 ensures the perturbation is in the linear stage.
- Dye calibration was performed using 0.01g/gal of Nigrosene dye in water, using a calibration wedge. The linear variation of pixel intensity with dye concentration for various background colors using the LED backlight was observed.
- Ensemble averaging of wide-field images of the mixing region was performed for about 300-600 images for each experiment, and mixing width, $2h$, was extracted from the contours of density. The 5% and 95% contours of volume fraction were used to calculate mixing width.
- Table 1 lists the set of experiments performed using single, binary and multi-mode ICs.
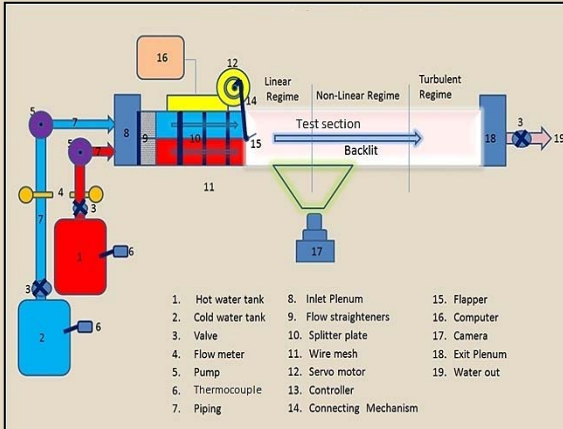- Density was measured from optical measurements and fast thermocouples (T-type at a sampling rate of 1kHz).
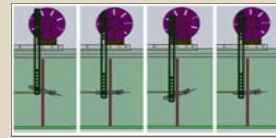

Fig. 2: Snapshots of flapper

Fig. 1: Schematic of experimental setup

1. Hot water tank
2. Cold water tank
3. Valve
4. Flow meter
5. Pump
6. Thermocouple
7. Piping
8. Inlet Plenum
9. Flow straighteners
10. Splitter plate
11. Wire mesh
12. Servo motor
13. Controller
14. Connecting Mechanism
15. Flapper
16. Computer
17. Camera
18. Exit Plenum
19. Water out

Table 1: List of experiments

IC Type	Case	λ_1 (cm)	λ_2 (cm)	λ_3 (cm)	β_1 (°)	β_2 (°)	A_t (× 10⁻³)
Single	1	0	-	-	-	-	1.28
	2	2	-	-	-	-	1.60
	3	4	-	-	-	-	1.83
	4	8	-	-	-	-	1.85
Binary	5	4	2	0	45	-	1.50
	6	4	4	0	45	-	1.81
	7	8	2	0	0	-	1.54
	8	8	2	0	45	-	1.63
	9	8	2	0	90	-	1.72
Multi	10	8	4	2	45	90	2.08
Binary	11	8	4	-	45	-	1.84

3a: With no flapper motion

3b: Single mode, $\lambda = 2$cm

3c: Single mode, $\lambda = 4$cm

3d: Single mode, $\lambda = 8$cm

32 in

12 in

3e: Binary mode, $(\lambda_1, \lambda_2) = (4, 2)$cm, $\beta = 45°$

3f: Binary mode, $(\lambda_1, \lambda_2) = (4, 4)$cm, $\beta = 45°$

3g: Ternary $(\lambda_1, \lambda_2, \lambda_3) = (8, 4, 2)$cm, $(\beta_1, \beta_2) = (45, 90)°$

3h: Binary mode, $(\lambda_1, \lambda_2) = (8, 2)$cm, $\beta = 0°$

3i: Binary mode, $(\lambda_1, \lambda_2) = (8, 2)$cm, $\beta = 45°$

3j: Binary mode, $(\lambda_1, \lambda_2) = (8, 2)$cm, $\beta = 90°$

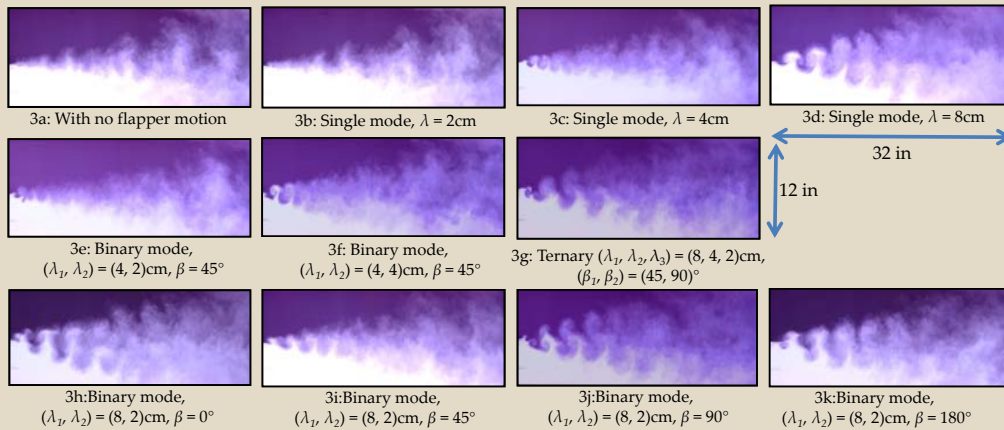3k: Binary mode, $(\lambda_1, \lambda_2) = (8, 2)$cm, $\beta = 180°$

Fig. 3: Flow visualization

Observations:

- Figure 3 shows the flow structures corresponding to the set of experiments, with enhanced contrast.
- Binary-mode bubbles and spike exhibit leaning with respect to the pressure gradient, similar to structures in Kelvin-Helmholtz instability (KHI). Variation of this leaning angle, γ, with phase angle, β, is being studied.
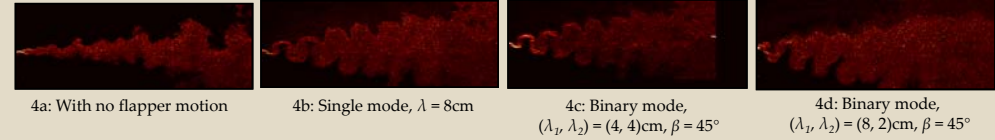

4a: With no flapper motion

4b: Single mode, $\lambda = 8$cm

4c: Binary mode, $(\lambda_1, \lambda_2) = (4, 4)$cm, $\beta = 45°$

4d: Binary mode, $(\lambda_1, \lambda_2) = (8, 2)$cm, $\beta = 45°$

Fig. 4: Pseudo Scalar dissipation, $\chi^* = D (\nabla \rho^* . \nabla \rho^*)/\nu$

- Contours of pseudo scalar dissipation using line-of-sight (LOS) images are presented in fig. 4 above. The pictures depict the variation of density gradients in different regions of the domain. Stronger gradients are observed near the splitter plate which weaken downstream. The strongest gradients are observed at the bubble fronts, for all experiments.
- Schmidt number, Sc, for dyed water ~1.0, therefore, pseudo- scalar dissipation is normalized with viscosity.
- Temperature profiles were taken at two stream-wise locations, $x = 1$ and 10inches, five span-wise locations, $y = -3, -1, 0, 1$ and 3inches and seven z-locations (each an inch apart).
- Density is calculated from temperature using a 5th order polynomial from densitometer measurements. Non-dimensional density or volume fraction of cold fluid $f_1 = \rho^* = (\rho (x, y, z, t) - \rho_h)/(\rho_c - \rho_h)$ is calculated. $f_2 = 1 - f_1$.
- Molecular mixing parameter, a measure of mixing due to molecular diffusion for two-fluid flows, is given by $\theta = 1 - B_0/B_2$, where $B_0 = (<\rho(x, y, z, t) - <\rho(x, y, z, t)>)^2/ (\rho_c - \rho_h)^2$ is the turbulent intensity of density fluctuations across the mixing layer in miscible fluids, and $B_2 = f_1.f_2$ is the molecular segregation for immiscible fluids. Here, $<>$ denotes the time mean.
- For validation of modified water channel. molecular mixing parameters are compared with previously published results for the water channel (Wilson and Andrews, Phys. Fluids, 2002 and Ramaprabhu & Andrews, J. Fluid Mech., 2003) shown below in fig. 5.
- Power spectra of ρ^* are also calculated at two downstream locations, i.e. $x/H = 0.077$ and $x/H = 0.908$ (corresponding to $t^* = 0.135$ and 1.621 respectively, shown in fig. 6 below.
- The slope of the power spectra, $B_0(\omega)$, between frequency $\omega = 10^{-2}$ and 10^{-3} varies with experiment and the location (x, y). There was insignificant variation of this slope with the spanwise-direction (z).
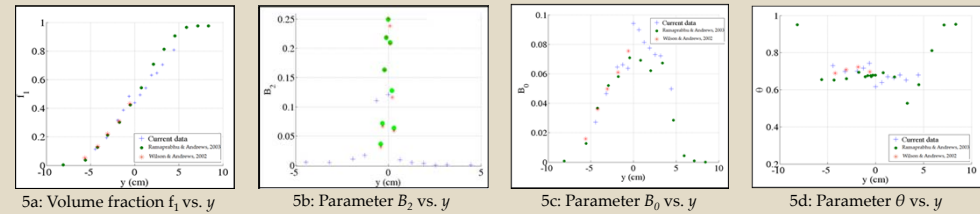

5a: Volume fraction f_1 vs. y

5b: Parameter B_2 vs. y

5c: Parameter B_0 vs. y

5d: Parameter θ vs. y

Fig. 5: Validation of molecular mixing data with previous experiments, at $x/H = 0.77$

6a: Spectrum vs. y at $x/H = 0.077$

6b: Spectrum vs. y at $x/H = 0.908$

6c: Spectrum vs. λ at $x/H = 0.077$

6d: Spectrum vs. λ at $x/H = 0.908$
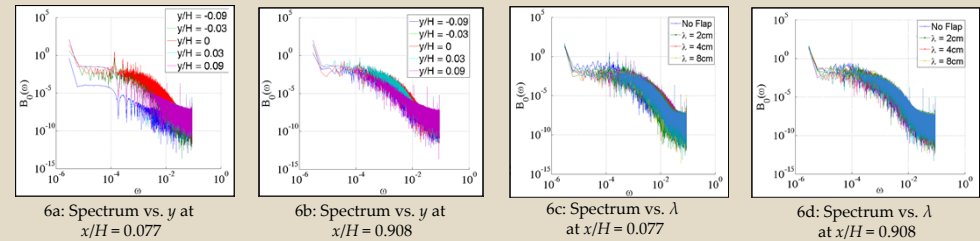
Fig. 6: Power spectra of ρ^* vs. y/H

S. No.	y/H	Case 1	Case 2	Case 3	Case 4	Case 5	Case 6	Case 7	Case 8	Case 9	Case 10
1	-0.23	-0.761	-0.732	-0.644	-2.041	-3.007	-2.858	-3.671	-3.276	-3.341	-3.311
2	-0.08	-2.893	-3.072	-2.965	-2.813	-2.353	-3.297	-3.711	-3.455	-3.033	--
3	0.00	-3.136	-3.113	-2.711	-2.508	-2.330	-3.019	-3.198	-2.970	-3.231	-3.651
4	0.08	-2.521	-2.245	-2.216	-2.133	-2.423	-2.960	-3.564	-3.307	-3.277	-3.591
5	0.23	-1.896	-1.848	-1.931	-1.856	-2.048	-2.178	-2.397	-2.281	-2.121	-2.230

Table 2: Slope of power spectra of ρ^* vs. y/H for all cases

Conclusions & Future work:

- Density measurements using optical techniques and thermocouples show variations in quantitative mixing (mixing width plots) and qualitative mixing (molecular mixing and slope of the power spectra of density) with initial condition.
- Buoyancy force causes anisotropic mixing and phase angle in initial condition causes shear-like behavior in the flow.
- Future measurements of velocity field are required (PIV is proposed) and effect of ICs on turbulent stage is also proposed.